Journal of Physics: Conference Series

Formation and decay of the Rydberg states of multiply charged ions interacting with solid surfaces

To cite this article: M A Mirkovi *et al* 2010 *J. Phys.: Conf. Ser.* **257** 012010

25th Summer School and International Symposium on the Physics of Ionized Gases—SPIG 2010 IOP Publishing
Journal of Physics: Conference Series **257** (2010) 012010 doi:10.1088/1742-6596/257/1/012010

Formation and decay of the Rydberg states of multiply charged ions interacting with solid surfaces

M. A. Mirković[1], N. N. Nedeljković[1], and D. K. Božanić[2]

[1] *University of Belgrade, Faculty of Physics, P.O. Box 368, Belgrade, Serbia*
[2] *Vinča Institute of Nuclear Sciences, P. O. Box 522, Belgrade, Serbia*

E-mail: gmirkomarko@sezampro.rs

Abstract. Processes of formation and decay of the Rydberg states of multiply charged ions escaping solid surfaces with intermediate velocities ($v \approx 1$ a.u.) represent complex quantum events that require a detailed quantum description. We have developed a two-state vector model for the population process, with the functions Ψ_1 and Ψ_2 for definition of the state of a single active electron. The electron exchange between the solid and the moving ion is described by a mixed flux through a plane positioned between them. For the low values of the angular momentum quantum numbers l the radial electronic coordinate ρ can be neglected, whereas for the large-l values a wide space region around the projectile trajectory was taken into account. The reionization of the previously populated states is considered as a decay of the wave function Ψ_2. The corresponding decay rates are obtained by an appropriate etalon equation method: in the large-l case the radial electronic coordinate ρ is treated as a variational parameter. The theoretical predictions based on that population-reionization mechanism are compared with the available beam-foil experimental data, as well as the experimental data obtained in the interaction of multiply charged ions with micro-capillary foil. Generally, the model reproduces the experimentally observed non-linear trend of the l distributions from $l = 0$ to $l_{\max} = n - 1$.

1. Introduction

It is well known that the Rydberg states of the multiply charged ions can be populated during the interaction with conducting solid surface. The beam-foil type of experiments [1-3] performed at intermediate velocities of the ionic projectiles ($v \approx 1$ a.u.), provide non-linear electron capture probability distributions for both principal and angular momentum quantum numbers, n and l, of the final bound states (n, l). Recently, a new type of experiment [4] for the multiply charged ions interacting with micro-capillary foils provided the evidence of the l distributions in the large-l region. A series of experimental data suggests that the formation of Rydberg states of multiply charged ionic projectiles escaping from solid surfaces represents a complex quantum event that can be considered as a specific interplay of the neutralization and reionization processes.

Most of the theoretical studies performed so far have not been focused on the cited experiments. The neutralization (electron capture) and ionization (recapture) are treated separately using rather different theoretical tools such as the classical over-barrier model [5, 6] and its extended dynamic version [7, 8], the standard perturbative quantum descriptions [9, 10], the non-perturbative coupled-angular-mode method [11], the complex scaling method [12], the stabilization method [13] and the time dependent close-coupling technique [14]. Recently, the wave packet propagation simulation [15, 16] has also been proposed. A common feature of

these models is the use of a single wave function for the description of the electron behavior at intermediate stages of the ion-surface interaction. Also, the models are devoted mainly to the low ionic velocities ($v \ll 1$ a.u.). On the other hand, the theoretical analysis [17] (classical transport theory) of the l distributions concerns the Rydberg-state population of multiply charged ions traversing foil bulk at high velocities ($v \gg 1$ a.u.).

In our theoretical treatment of the process, two specific models are used for the population of the low-l and the large-l Rydberg states, and both the neutralization and reionization are taken into account. The probability distributions for the low-l Rydberg states ($l = 0, 1$ and 2) have been obtained within the framework of two-state-vector model (TVM) [18, 19]. The model has also been extended to the case of large-l Rydberg states ($l \geq 3$) [20]. Using the TVM, our prime intention has been to learn information about the behavior of the active electron which left the solid surface at the time t_{in}, but which will be detected in the final bound state (n, l) at the time t_{fin}. To this end, we describe the single active electron simultaneously using the wave function $\Psi_1(\vec{r}, t)$, evolving from a fixed initial state, and an additional "teleological" wave function $\Psi_2(\vec{r}, t)$, evolving causally towards a fixed final state (n, l) of the ionic projectile [18-23]. In particular, such a description is relevant for the intermediate velocity region ($v \approx 1$) where the adiabatic approximation breaks down [18, 19]. Also, the concept of the mixed flux through the moving "Firsov plane" S_F, used in the calculation of the transition probabilities, offers the possibility to treat the functions $\Psi_1(\vec{r}, t)$ and $\Psi_2(\vec{r}, t)$ in the "interaction-free" region which is far from both the ion and the surface, for large ion-surface distances R. As a result we obtain the intermediate neutralization probabilities $P^N_{\nu_A}(t)$ and neutralization rates $\Gamma^N_{\nu_A}(t)$, where ν_A is the set of the intermediate spherical quantum numbers.

In the Refs. [18], [19] and [20] we considered the electron exchange exclusively as an electron capture from the foil conduction band into the moving Rydberg state (n, l) of the ionic projectile, i.e., the reionization was neglected. In few cases the experimental lower-n values of the electron capture probability $P_{nl} = \lim_{t \to t_{fin}} P^N_{\nu_A}(t)$ near $l = l_{max} = n - 1$ have been overestimated by the proposed model. Moreover, in the case of larger-n states the theory predicted an oscillatory l-behavior of the P_{nl} curves with large amplitudes in the large-l region. Just in this region, the absence of the experimental data in the beam-foil geometry [1, 2, 3] has been previously considered as the existence of the thresholds at $l = l_{thr} < l_{max}$. However, the new experiments with microcapilary foil [4] give the nonzero population probabilities in this region, but with lower values then those obtained in the cited TVM.

The limitations of the TVM are removed by taking into account the fact that the electron capture process is in competition with the reionization at intermediate stages of the ion-surface interaction. Effects of reionization in the low-l case have been included in the population process in Ref. [22]. The reionization of the large-l Rydberg states can be described by the same method as in the low-l case: the wave function $\Psi_2(\vec{r}, t)$ has to be "renormalized", i.e., multiplied by the corresponding decay factor $\mathcal{E}_{\mu_A}$, where μ_A denotes the set of intermediate parabolic quantum numbers (which give the main contribution to the electron capture process) [20],[22]. The decay factor $\mathcal{E}_{\mu_A}$ is expressed via the ionization rate $\Gamma^I_{\mu_A}$, which is calculated using the complex eigenenergy model combined with the etalon equation method (EEM). The parabolic symmetry in the low-l case appears as a consequence of the fact that the radial electronic coordinate ρ can be neglected in comparison to the ion-surface distance R. In contrast to the low-l case, in the case of large-l Rydberg states, the electron transitions are mainly localized far from the ionic trajectory. Within the framework of the large-l EEM, the quantity ρ is considered as a variational parameter; the parabolic symmetry is preserved in this procedure. Using the large-l reionization rate $\Gamma^I_{\mu_A}$, we calculate the relevant decay factor $\mathcal{E}_{\mu_A}$, from which the experimentally verifiable "renormalized" population probabilities $\overline{P}_{nl} = \mathcal{E}^2_{\mu_A} P_{nl}$ can be find.

2. The renormalized population probabilities $\overline{P}_{nl}$

2.1. The population-reionization mechanism

We consider the population-reionization (capture-recapture) process for Rydberg states of multiply charged ions escaping solid surfaces with velocity v, Fig 1(a).

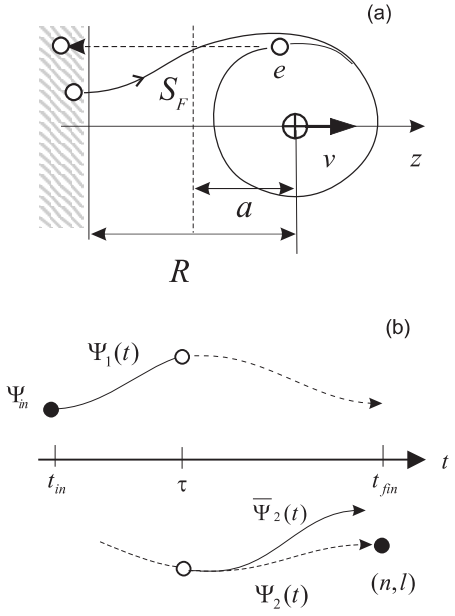

Figure 1. (a) Schematic description of the population-reionization mechanism for the Rydberg states of multiply charged ions escaping the solid surface and (b) the corresponding TVM-scheme. The spherical shape of the formed Rydberg state corresponds to the large-l case. In the low-l case the electronic state is characterized by the large eccentricity. In the large-l case the neutralization process (electron capture from the solid into the ionic field) can be suppressed by the reionization (electron recapture by the solid). Accordingly, if the reionization is remarkable, only a fraction of the formed Rydberg states survives and can be detected as a final state (n, l) at the time $t = t_{fin}$. The reionization and neutralization processes begins practically at the same ion-surface distances, $R = R_\tau \approx R_g$.

The process under consideration has the following TVM interpretation [20, 22, 23], Fig. 1(b). The state $\Psi_1(\vec{r}, t)$ evolves from an initial state Ψ_{in} labeled by the set of parabolic quantum numbers $\mu_{M,in}$ at the time $t_{in} = 0$. The population process represents a "transition" $\Psi_1(\vec{r}, t) \to \Psi_2(\vec{r}, t)$ at the intermediate time $t \in (t_{in}, t_{fin})$. If the reionization could be neglected, the state $\Psi_2(\vec{r}, t)$ would evolve into a final bound state determined by the spherical quantum numbers $\nu_{A,fin} = (n, l, m)$ at the time $t_{fin} \to \infty$. The reionization is included in the model by introducing the "renormalized" wave function $\overline{\Psi}_2(\vec{r}, t) = \mathcal{E}_{\mu_A}(t)\Psi_2(\vec{r}, t)\Theta(z) + \chi(\vec{r}, t)\Theta(-z)$ for $t > \tau$, where $\tau = R_\tau/v$ [22]. For $t < \tau$ we take $\overline{\Psi}_2(\vec{r}, t) = \Psi_2(\vec{r}, t)$. The regions inside and outside the solid ($z < 0$ and $z > 0$) are defined by the Heaviside function $\Theta(z)$. The function $\chi(\vec{r}, t)$ stands for the outgoing wave inside the solid.

The state $\overline{\Psi}_2$ represents a decaying state, with a decay factor

$$\mathcal{E}_{\mu_A}(t) = \exp\left[-\frac{1}{2}\int_\tau^t \Gamma^I_{\mu_A}(t)dt\right], \tag{1}$$

where $\Gamma^I_{\mu_A}(t)$ is the reionization rate for the relevant intermediate parabolic quantum numbers $\mu_A = \{n_1 = 0, n_2 = n - 1, m = 0\}$. The experimentally verifiable renormalized population probability $\overline{P}_{nl}$ is given by [22]

$$\overline{P}_{nl} = \mathcal{E}^2_{\mu_A} P_{nl}, \tag{2}$$

where $\mathcal{E}^2_{\mu_A} = \lim_{t\to\infty} \mathcal{E}^2_{\mu_A}(t)$, whereas P_{nl} represents the electron capture probability (without reionization) into the final Rydbeg state (n, l).

2.2. Calculation of P_{nl}

In order to calculate the population probability P_{nl} within the framework of TVM, we define the two-state probability amplitude $A_{\mu_M,\nu_A}(t) = \langle\Psi_2(t)|\hat{P}_A(t)|\Psi_1(t)\rangle$, where $\hat{P}_A(t) = \int_{V_A} |\vec{r}_A\rangle\langle\vec{r}_A|dV$ is the projection operator onto the ionic region $V_A = \{z; z \geq R - a\}$, see Fig. 1(a), and calculate

the intermediate neutralization probability $P^N_{\nu_A}(t)$; the final probability P_{nl} follows for $t \to \infty$ [20, 23].

The intermediate neutralization probability $P^N_{\nu_A}(t)$ is defined as an integral over the solid conduction band energy parameter γ_M and a sum over the first parabolic quantum number n_{1M} and magnetic quantum number m_M of the quantity $|A_{\mu_M,\nu_A}(t)|^2$:

$$P^N_{\nu_A}(t) = \int \sum_{n_{1M},m_M} |A_{\mu_M,\nu_A}(t)|^2 d\gamma_M. \tag{3}$$

The two-state probability amplitude can be expressed via mixed flux $I_{\mu_M,\nu_A}(t)$ through the Firsov plane S_F (with surface element $d\vec{S}$) separating the region V_A from the complementary region:

$$A_{\mu_M,\nu_A}(t) = \int_{t_g=R_g/v}^{t} I_{\mu_M,\nu_A}(t)dt, \tag{4}$$

$$I = \frac{i}{2}\int_{S_F}\left[\frac{\vec{\nabla}\Psi_1}{\Psi_1} - \frac{\vec{\nabla}\Psi_2^*}{\Psi_2^*} - 2i\vec{v}\left(1-\frac{da}{dR}\right)\right]\Psi_2^*\Psi_1 \cdot d\vec{S}. \tag{5}$$

The kinematics of the Firsov plane is determined by the variational requirement $\delta P_{\nu_A}(t)/\delta a(t) = 0$ where $a = a(t)$ is the position of the S_F plane with respect to the ion. The former condition reflects the fact that the probability $P^N_{\nu_A}(t)$ should be independent of the small variations of the S_F plane position.

The wave functions Ψ_1 and Ψ_2 can be expressed as space-time modifications of the eigenfunctions Φ_{MA,μ_M} and Φ_{AM,ν_A} of the Hamiltonians $\hat{H}_i$, $i = 1, 2$, of the first and second scenarios, respectively [18, 19, 23]: $\Psi_1(\vec{r},t) = \Phi_{MA,\mu_M}\exp\left(f_M + i\gamma_M^2 t/2\right)$ and $\Psi_2(\vec{r},t) = \Phi_{AM,\nu_A}\exp\left(ivz - iv^2t/2\right)\exp\left(f_A + i\gamma_A^2 t/2\right)$. By $f_M = f_M(\vec{r},t)$ and $f_A = f_A(\vec{r},t)$ we denoted the corresponding correction factors, whereas $\exp(ivz - iv^2t/2)$ represents the Galilei factor. The explicit expressions of the eigenfunctions Φ_{MA,μ_M} and Φ_{AM,ν_A}, and the correction factors f_M and f_A are obtained using the different asymptotic methods for the low-l ($l = 0, 1, 2$) and the large-l ($l \geq 3$) cases.

Considering the electron capture into the low-l Rydberg states [18, 19, 23], it is plausible to assume that the mixed flux through the central part of the Firsov plane give the main contribution to the transition amplitude. That is, in the low-l case the ionic Rydberg states have large eccentricities so that only a narrow cylindrical region around the ionic trajectory becomes relevant. The functions $\Psi_1(\vec{r},t)$ and $\Psi_2(\vec{r},t)$ are obtained by an analytic continuation from the regions where they are mainly localized (the solid region and the ionic region, respectively) to the central part of the Firsov plane. A generalization of the low-l TVM to the large-l Rydberg systems has been performed in Ref. [20]. Taking into account that the large-l Rydberg states are characterized by very small eccentricities it was assumed that the relevant area of the Firsov plane extends far from the ionic trajectory. This fact has been taken into account in the calculation of the wave function $\Psi_1(\vec{r},t)$; namely, the JWKB form of the function Φ_{MA,μ_M} (analytically continued from the metallic region into the ionic region) valid in the central part $\rho \approx 0$ of the S_F plane is "bifurcated" on the whole Firsov plane by the appropriate matching procedure.

2.3. Calculation of $\mathcal{E}_{\mu_A}$

From Eq. (1) we see that the problem of reionization characteristic for the population of the large-l Rydberg states is reduced to the evaluation of the decay factor $\mathcal{E}_{\mu_A}(t)$, i.e., the rate $\Gamma^I_{\mu_A}(t)$.

By considering the complex energy eigenvalue problem of the of the Hamiltonian $\hat{\overline{H}}_2(t)$

$$\hat{\overline{H}}_2(t)\Phi_{AM,\mu_A} = E_A\Phi_{AM,\mu_A}, \tag{6}$$

one get the energies

$$E_A(R) = \mathrm{Re}E_A(R) - i\Gamma^I_{\mu_A}(t)/2; \tag{7}$$

from the imaginary part of the energies E_A we obtain, directly, the parabolic ionization rates $\Gamma^I_{\mu_A}$. The Hamiltonian $\hat{\overline{H}}_2$ differs from the final-channel Hamiltonian $\hat{H}_2$ used in the absence of reionization by the term $-U_0\Theta(-z)$, where U_0 is the depth of the potential well of the solid. The appropriate method of solving the eigenvalue problem expressed by Eq. (1) is the EEM.

The parabolic symmetry of the eigenvalue problem (8) in the low-l case appeared as a consequence of the fact that the radial electronic coordinate ρ could be neglected in comparison to the ion-surface distance R [22]. In contrast to the low-l case, in the case of large-l Rydberg states the electron transitions are mainly localized far from the ionic trajectory. In that case the parabolic symmetry is preserved for the quantity $\rho = \bar{\rho}$ treated as a variational parameter. The problem of calculation of the corresponding rate $\Gamma^I_{\mu_A}(t)$ can be performed in two steps. In the first step we calculate the rates $\Gamma^I_{\mu_A}(\bar{\rho}, R)$ with $\bar{\rho}$ as a parameter. In the next step, we calculate the quantity $\bar{\rho} = \bar{\rho}_0(\mu_A; R)$ using the variational requirement: $\delta\Gamma^I_{\mu_A}(\bar{\rho}, R)/\delta\bar{\rho} = 0 \Leftrightarrow \bar{\rho} = \bar{\rho}_0(\mu_A; R)$. In that way we obtain the rates $\Gamma^I_{\mu_A}(\bar{\rho}_0(\mu_A; R), R) = \Gamma^I_{\mu_A}(t)$. The low-$l$ results follow as a limiting case $\bar{\rho} \to 0$ of large-l case.

With the parabolic symmetry preserved, one can separate the variables in Eq. (8) in parabolic coordinates $\xi = r_A + z_A$, $\eta = r_A - z_A$ and φ, where the index "A" is addressed to the quantities defined in the coordinate system located at the ionic core. Bearing in mind the relation $\rho^2 = \xi\eta$, we get two one-dimensional effective eigenvalue problems (along the ξ and along the η directions), which both depend on the variational parameter $\bar{\rho}$. The large-l intermediate Rydberg system (formed in the neutralization process) is almost spherical and large; thus, its reionization is related to electron transitions far from the ionic trajectory ($\bar{\rho}_0 \gg 1$). The effective one-dimensional problems of the low-l reionization model [22] follow in the limit $\bar{\rho} \to 0$ from the corresponding large-l expressions. In both cases we use the scaled parabolic coordinates $\tilde{\xi} = \xi/2R\alpha_\xi$, $\tilde{\eta} = \eta/2R\alpha_\eta$ and φ, in order to obtain the canonical forms of the one-dimensional eigenvalue problems suitable for application of the EEM. We note that the scaling parameters α_ξ and α_η are different in the large-l and the low-l cases.

2.4. The final population probability $\overline{P}_{nl}$ and comparison with experiment

The electron exchange during the intermediate stages of the ion-surface interaction results in the formation of the final Rydberg system (n, l) at $t_{fin} \to \infty$. The experimentally verifiable population probability $\overline{P}_{nl}$, Eq. (2), can be calculated explicitly for all relevant values of the ion-surface parameters. The theoretical predictions are be compared with available experimental data for the ions ClVII and ArVIII. In presenting the theoretical results we shall focus on the l distributions, using the same normalization of the experimental data as in Ref. [20].

In Figs. 2 and 3 we present the renormalized population probabilities $\overline{P}_{nl}$ obtained by inclusion of the reionization (full curves) and the probabilities P_{nl} (dashed curves) [19],[20] for the ions ClVII (core charge $Z = 7$) and ArVIII (core charge $Z = 8$) with $7 \le n \le 12$ escaping the solid surface at velocity $v = 2.50$ a.u. and $v = 1.42$ a.u., respectively. The pronounced peaks of the P_{nl} distributions in the large-l region are lowered due to the reionization; note the existence of the threshold value $n = n_{thr} = 9$ in the low-l region, i.e. $P_{nl} = 0$ for $n > n_{thr}$ in the case of ClVII. The properly normalized beam foil experimental data from Ref. [1, 2] and Ref. [3] for ClVII and ArVIII ions, respectively, are presented by dots.

The experimental data for neutralization of the Ar^{7+} ion ($Z = 7$), and Ar^{8+} ion ($Z = 8$) obtained in the presence of microcapillary foil [4] are presented by circles. The available experimental data [4] are for $v \approx 0.2$ a.u., so that the experimental results are scaled to the intermediate velocity case (and properly normalized). We recognize that the proposed renormalized TVM predictions are in agreement with both sets of available experimental data.

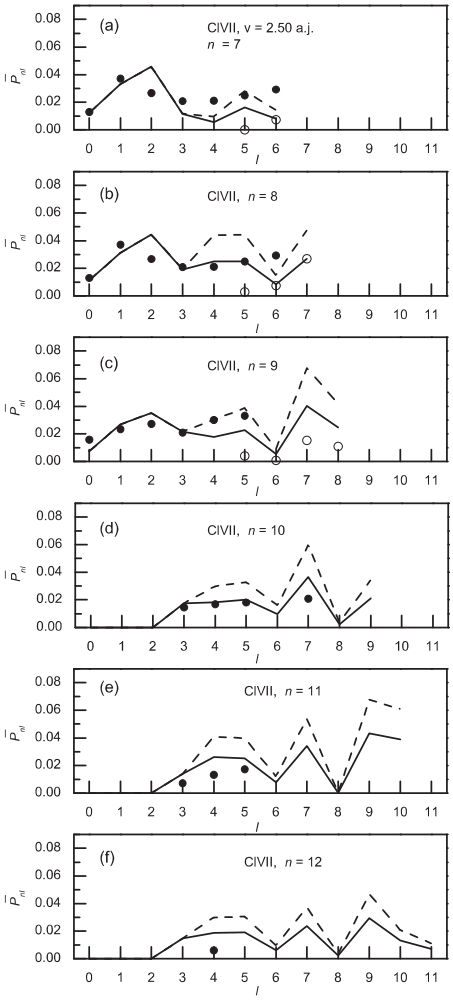

Figure 2. Renormalized population probabilities $\overline{P}_{nl}$ (full curves) and population probabilities P_{nl} (dashed curves) for the ClVII ion, via angular momentum quantum number l, for $7 \leq n \leq 12$, and $v = 2.50$ a.u. The low-l probabilities P_{nl} are from Ref. [19] and the large-l values P_{nl} are from Ref. [20]. Dots and circles are the beam-foil [1, 2] and the beam-microcapillary foil experimental data [4], respectively.

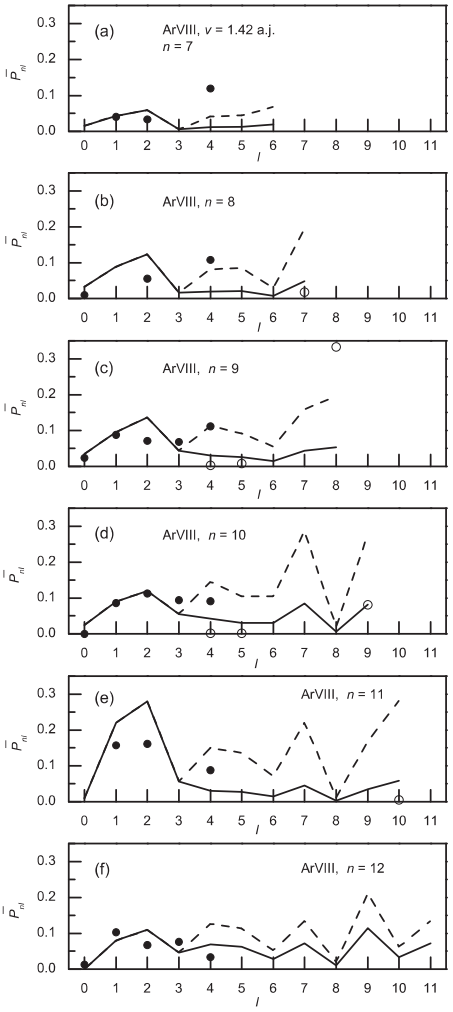

Figure 3. Renormalized population probabilities $\overline{P}_{nl}$ (full curves) and population probabilities P_{nl} (dashed curves) for the ArVIII ion, via angular momentum quantum number l, for $7 \leq n \leq 12$, and $v = 1.42$ a.u. The low-l probabilities P_{nl} are from Ref. [19] and the large-l values P_{nl} are from Ref. [20]. Dots and circles are the beam-foil [3] and the beam-microcapillary foil experimental data [4], respectively.

3. Concluding remarks

By the analysis presented in this article we complete our discussion of the l population distributions for the Rydberg states of multiply charged ions, for $v \approx 1$ a.u. The low-l [18, 19] and the large-l, but lower-n [20] studies have been performed within the framework of the TVM. The reionization mechanism [22] is adapted to the large-l case and also included in the model. The population distributions are obtained, which reflect the n- and l- selective

population character, in agreement with both sets of available experiments: the beam-foil [1-3] and the beam-microcapillary foil [4] experiments.

Few additional concluding comments may be relevant for further extension of the presented theoretical approach.

First, in the presented model all ionic projectiles have been considered as point-like. The more realistic description of the ionic core, with core polarization effectively taken into account, can be included into the population/reionization model, using the modified wave function Ψ_2 [24, 25]. Second, the electron transitions in the very vicinity of the potential barrier top can be considered more accurately, like in Ref. [26]. Third, we found that the l distributions for the Rydberg states of multiply charged ions are very sensitive with respect to the ionic velocities. This circumstance can be used to test if the Rydberg states are formed inside the bulk of the foil, or over the surface, along the outgoing part of the ionic trajectory. It is possible to estimate upper velocity limits for the population-reionization process considered as a surface phenomenon.

Finally, we note that the experiments analyzed in this report were not designed for a direct observation of the quantum events at intermediate stages of ion-surface interaction. Therefore, comparing our theoretical data with the cited experiments, we only indirectly demonstrated the relevance of the reionization. The experimental evidence about the intermediate stages of the process will be of interest.

Acknowledgments
This work was supported in part by the Ministry of Science and Technological Development, Republic of Serbia (Project 14 1029).

References

[1] Veje E 1985 *Nucl. Instrum. Methods Phys. Res.* B **9** 586
[2] Veje E and Winter H *Z. Phys.* D **10** (1988) 457
[3] Bashkin S, Oona H and Veje E 1982 *Phys. Rev.* A **25** 417
[4] Morishita Y, Hutton R, Torri H, Komaki K, Brage T, Ando K, Ishii K, Kanai Y, Masuda H, Sekiguchi M, Rosmej F B and Yamazaki Y 2004 *Phys. Rev.* A **70** 012902.
[5] Burgdörfer J in *Review of Fundamental Processes and Applications of Atoms and Molecules* ed by C.D. Lin (World Scientific, Singapore,1993)
[6] Burgdörfer J, Lerner P and Meyer F W 1991 *Phys. Rev.* A **44** 5674
[7] Ducrée J J, Casali F and Thumm U 1998 *Phys. Rev.* A **57** 338
[8] Ducrée J J, Andrä H J and Thumm U 1999 *Phys. Rev.* A **60** 3029
[9] Wille U 1994 *Phys. Rev.* B **50** 1888
[10] Kürpick P and Thumm U 1996 *Phys. Rev.* A **54** 1487
[11] Borisov A G, Zimny R, Teillet-Billy D and Gauyacq J P 1996 *Phys. Rev.* A **53** 2457
[12] Nordlander P 1996 *Phys. Rev.* B **53** 4125
[13] Deutscher S A, Yang X and Burgdörfer J 1995 *Nucl. Instrum. Methods Phys. Res.* B **100** 336
[14] Kürpick P, Thumm U and Wille U 1998 *Phys. Rev.* A **57** 1923
[15] Sjakste J, Borisov A G and Gauyacq J P 2006 *Phys. Rev.* A **73** 042903
[16] So E, Bell M T and Softley T P 2009 *Phys. Rev.* A **79** 012901
[17] Kemmler J, Burgdörfer J and Reinhold C O 1991 *Phys. Rev.* A **44** 2993
[18] Nedeljković N N, Nedeljković Lj D, Vojvodić S B and Mirković M A 1994 *Phys. Rev.* B **49** 5621
[19] Nedeljković Lj D and Nedeljković N N 1998 *Phys. Rev.* B **58** 16455
[20] Nedeljković N N, Nedeljković Lj D and Mirković M A 2003 *Phys. Rev.* A **68** 012721
[21] Nedeljković N N, Nedeljković Lj D, Janev R K and Mišković Z L 1991 *Nucl. Instrum. Methods Phys. Res.* B **58** 519
[22] Nedeljković Lj D and Nedeljković N N 2003 *Phys. Rev.* A **67** 032709
[23] Nedeljković N N and Majkić M D 2007 *Phys. Rev.* A **76** 042902
[24] Nedeljković N N, Majkić M D, Galijaš S M D and Mitrović S B 2008 *App. Surf. Sci.* **254** 7000
[25] Nedeljković N N, Galijaš S M D and Majkić M D 2009 *Surf. Sci.* **603** 2403
[26] Nedeljković Lj D, Nedeljković N N and Božanić D K 2006 *Phys. Rev.* A **74** 032901